Journal of Medicinal Chemistry

Article

pubs.acs.org/jmc

1,7-Naphthyridine 1-Oxides as Novel Potent and Selective Inhibitors of p38 Mitogen Activated Protein Kinase†

Wenceslao Lumeras,[‡,#] Laura Vidal,[‡] Bernat Vidal,[‡] Cristina Balagué,[§] Adelina Orellana,[§] Mónica Maldonado,[§] María Domínguez,[∥] Víctor Segarra,[⊥] and Francisco Caturla*[,‡]

[‡]Department of Medicinal Chemistry, [§]Department of Biology, [∥]Department of ADME, and [⊥]Department of Computational and Structural Drug Discovery, Almirall Research Center, Almirall S.A., Ctra. Laureà Miró 408, E-08980 Sant Feliu de Llobregat, Barcelona, Spain

Supporting Information

ABSTRACT: The design, synthesis, and ability to inhibit p38α MAP kinase by a novel series of naphthyridine *N*-oxides will be described. Some of these compounds showed a significant reduction in the LPS-induced TNFα production in human whole blood. Structure−activity relationship studies revealed that *N*-oxide oxygen was essential for activity and was probably a determinant factor for its marked selectivity against other related kinases. After an extensive SAR exercise, several compounds from this series were identified as very potent p38α inhibitors. In vivo efficacy of some derivatives was demonstrated to reduce TNFα levels in an acute murine model of inflammation (ED_{50} = 0.5 mg/kg in LPS-induced TNFα production when dosed orally 1.5 h prior to LPS administration). The oral efficacy was further demonstrated in a chronic model of adjuvant arthritis in rats with established disease when administered orally (ED_{50} < 1 mg/kg).

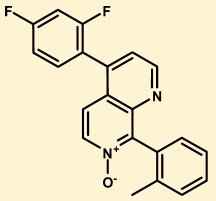

p38α IC_{50} = 68 nM

Panel of 54 Tyrosine and Serine/Threonine Kinases IC_{50} > 10 μM

INTRODUCTION

The p38α mitogen activated protein (MAP) kinase is an intracellular serine/threonine (Ser/Thr) kinase that is activated by a range of environmental stimuli such as TNFα, IL-1β, and stress.[1,2] Activation of p38α occurs through bisphosphorylation by the dual-specificity Ser/Thr MAP kinases MKK3 and MKK6 on the Thr180-Gly181-Tyr182 motif located on the activation loop.[2,3] In its activated state, p38α phosphorylates a range of intracellular protein substrates that post-transcriptionally regulate the biosynthesis of TNFα and IL-1β. The pathophysiological consequence of excessive production of TNFα and IL-1β is thought to be significant mediation of the progression of many inflammatory diseases such as rheumatoid arthritis, psoriasis, and inflammatory bowel disease.[4−7] The inhibition of p38α MAP kinase can efficiently regulate both the release and the activity of those proinflamatory cytokines, and it has been seen as an opportunity to discover novel anti-inflammatory drugs.[8]

Since the first report in 1994 of the pyridylimidazole-based p38α inhibitor SB203580,[9] a variety of compounds have advanced into clinical trials for rheumatoid arthritis, reaching proof-of-concept phase.[10] The robust preclinical validation of the target along with the reported efficacy for VX-745[11,12] spurred the conceptualization of novel p38 MAPK inhibitors with improved pharmacological profiles. As of today, there is scarce information on the clinical results obtained for the most advanced compounds in rheumatoid arthritis, although a recent report on pamapimod has unveiled a transient reduction in inflammation that may have compromised overall efficacy.[13]

As part of our strategy to identify novel, potent, and selective p38α MAP kinase inhibitors, we focused our interest in the unprecedented level of selectivity shown by ligands that display a simultaneous double interaction with the backbone amide NH of Met109 and Gly110.[14] In this sense, we selected two starting points for our rational design: Merck inhibitor **1** (Figure 1a)[15] and aminopyridine *N*-oxide **2** (Figure 1b).[16] Merck inhibitor **1** is derived from a dihydroquinolinone core[17,18] and is characterized by the presence of two pendent aromatic rings that are critical for the enzymatic potency. This p38α MAP kinase inhibitor displayed potent activity (p38α IC_{50} = 0.74 nM) and selectivity for p38α over a variety of other closely related kinases, including ERK1 and JNK1−3 (>10000 fold).[15] On the other hand, aminopyridine *N*-oxide **2**, that was derived from Bayer p38α inhibitor pyridinones,[9,20] is also a potent (p38α IC_{50} = 21 nM) and selective p38α inhibitor. The X-ray crystal structure of these two compounds cocrystallized with unphosphorylated p38α[15,16] revealed the formation of two key hydrogen bond contacts between an oxygen atom of the ligands (carbonyl for **1** and *N*-oxide for **2**) and the backbone amide NH of Met109 and NH of Gly110, inducing a conformational change in the hinge region of the enzyme ("Gly flip"). Moreover, both molecules show a fine-tuned occupation of the hydrophobic pocket I placed near the gatekeeper Thr106. Overlaying X-ray crystal structures of **1** and **2** clearly revealed the similarities of the key hydrogen bond interactions of both compounds with the hinge region of the enzyme, strengthening the pseudobicyclic disposition of aminopyridine *N*-oxides through the formation of an intramolecular hydrogen bond between the carbonyl oxygen and the amino group and placing the pendent aryl rings of **2** in a

Received: July 21, 2011
Published: October 14, 2011

ACS Publications © 2011 American Chemical Society

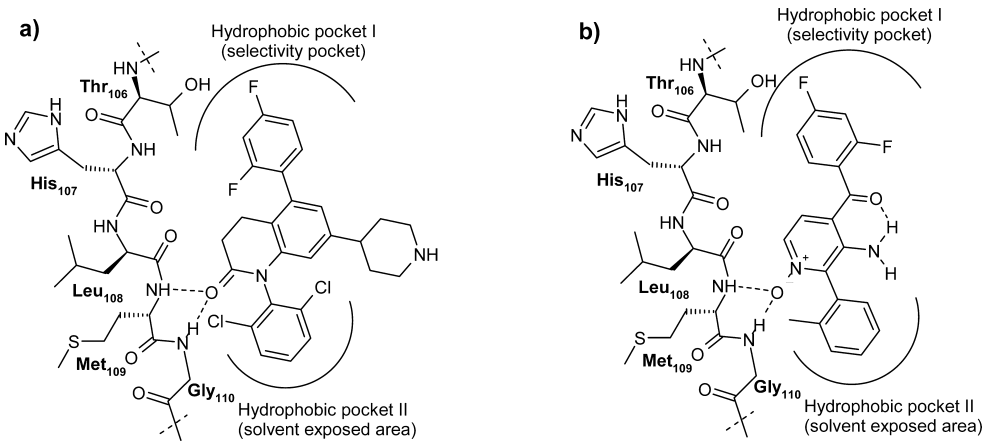

Figure 1. (a) Schematic representation of key interactions of the dihydroquinolinone-based Merck's inhibitor **1** in the active site of p38α, derived from X-ray complex 1OVE.[15] (b) Schematic representation of key interactions of aminopyridine *N*-oxide inhibitor **2** in the active site of p38α, derived from X-ray complex 3HRB.[16]

conformation similar to that of **1** within the p38α active site (Figure 1).

In light of these two crystal structures, we assume that the exquisite selectivity of these compounds relays an optimum interaction with the hydrophobic pocket I, which is particularly accessible in p38α because of the size of the gatekeeper amino acid (Thr106), as well as the ability of the ligands to force a Gly flip, which is an almost exclusive feature of p38α. Other related kinases contain bulkier residues at this position, which makes the conformational change virtually impossible,[14] giving some explanation to the high degree of selectivity achieved by compounds **1** and **2**.

With the aim of identifying novel, potent, and selective p38α inhibitors based on the X-ray studies of these structures in the catalytic site of the enzyme, a bicyclic core **B** emerged as a logical step forward from **A** in the design of conformationally more rigid analogues, keeping the unique binding mode through the *N*-oxide oxygen atom (Figure 2). Additionally,

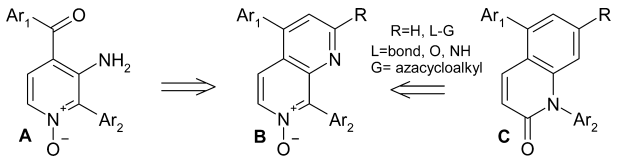

Figure 2. Derivation of the novel naphthyridines *N*-oxide core **B**.

Merck's quinolinones **C** confirmed that a bicyclic core could provide access to good p38α inhibitors, and therefore, we propose naphthyridine *N*-oxides **B** as a suitable integrated alternative.

CHEMISTRY

Naphthyridines **3**–**20** (R^3 = H) were prepared by a variant of the Friedländer cyclization[a] following the synthetic route depicted in Scheme 1. Starting from the corresponding aminopyridines,[16] the cyclization with acetaldehyde was carried out using microwave irradiation in glacial AcOH. In the case of R^3 substituted naphthyridines ($R^3 \neq$ H) **21**, **22**, **25**–**28**, the optimum conditions for the cyclization of the starting aminopyridines with the corresponding methylketones consist of the combination of acid catalysis (concentrated H_2SO_4) and a desiccant ($MgSO_4$).

Scheme 1[a]

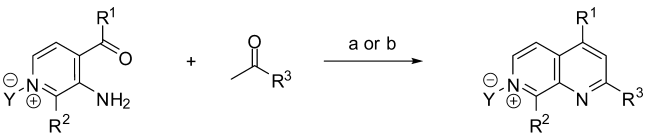

37a-s **3-22, 25-28**

[a]Reagents and conditions: (a) (R^3 = H) AcOH glacial, microwave, 100 °C, 32–85%; (b) ($R^3 \neq$ H) H_2SO_4 conc, $MgSO_4$ anh, PhMe, 115 °C, 32–73%.

Regarding the piperidine substituted naphthyridines, some of them were derivatized on the piperidine nitrogen (alkylation/acylation), as depicted in Scheme 2, to afford compounds **23**, **24**, and **29**.

Scheme 2[a]

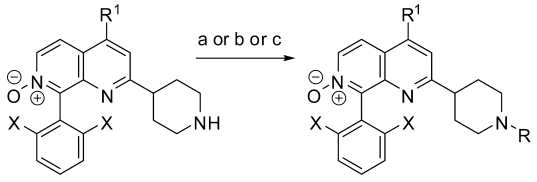

21, R1=2,4-diF-Ph; X=Cl
22, R1=2-Cl,4-F-Ph; X=Cl
28, R1=2-Cl-Ph; X=F

23, R1=2-Cl,4-F-Ph; X=Cl; R=Me
24, R1=2-Cl,4-F-Ph; X=Cl; R=iPr
29, R1=2-Cl-Ph; X=F; R=Ac

[a]Reagents and conditions: (a) (R = Me, **23**) HCHO, HCOOH, 80 °C; (b)(R = ^{i}Pr, **24**) ^{i}PrBr, KI, K_2CO_3, ACN, 80 °C; (c) (R = Ac, **29**) AcCl, Et_3N, CH_2Cl_2.

For the preparation of R^3 substituted naphthyridines **30**–**36**, having a heteroatom as the attachment point with the naphthyridine core, we followed the synthetic pathway shown in Scheme 3. The amino group of the corresponding aminopyridines **38a**–**c**[16] was acylated with pivaloyl chloride. Subsequent addition of the *tert*-butyl acetate enolate over the diaryl ketone group furnished an intermediate that was submitted to acidic cyclization affording naphthyridinones **39a**–**c**. These intermediates were converted into the corresponding *N*-oxides **40a**–**c** via a smooth oxidation with *m*CPBA, and the latter compounds were treated with $POCl_3$ to install a chlorine atom at position 2 of the naphthyridine

dx.doi.org/10.1021/jm200975u | J. Med. Chem. 2011, 54, 7899–7910

Scheme 3[a]

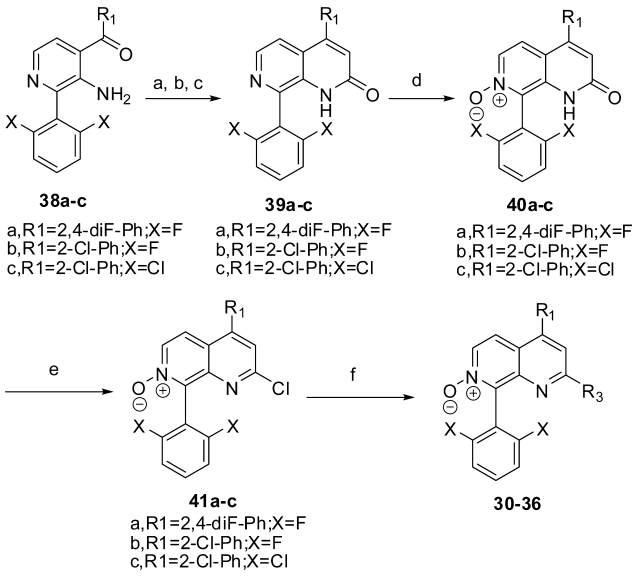

[a]Reagents and conditions: (a) pivaloyl chloride, DIEA, dioxane, 110 °C; (b) LDA, AcOtBu, THF, −78 °C; (c) HCl, 100 °C; (d) *m*CPBA, CH_2Cl_2, room temp; (e) $POCl_3$, 110 °C; (f) R^3H, base, 110−130 °C.

system. The introduction of different R^3 groups was done by nucleophilic displacement of the chlorine atom, affording the desired naphthyridines **30**−**36**.

RESULTS AND DISCUSSION

In light of the high similarity of the bicyclic core design with the already studied aminopyridine series,[16] we followed the main part of the trends identified in that series in order to speed up the naphthyridines SAR exploration. Taking into account that the putative non-*N*-oxide aminopyridines retained a considerable inhibitory potency, we considered it interesting to test the potency of the corresponding non-*N*-oxide naphthyridines. In this sense, naphthyridine **3** (Table 1) showed some degree of p38α inhibition in the micromolar range, similar to that in the aminopyridine series but far from the potency conferred by the *N*-oxide group, as we will see next.

Subsequently, we oxidized the nitrogen on the 7 position. This oxygen atom would be responsible for the postulated interactions with the hinge region, affording compound **4** with a reasonable inhibitory potency (p38α IC_{50} = 68 nM) in the enzymatic assay. We considered this initial value as the proof-of-concept of our bicyclic core design, and preliminary SAR expansion of this series was undertaken to further explore its full potential. Following the same exploratory sequence as in the former aminopyridine series, we started to explore the best occupation of the hydrophobic pocket II (Figure 1). We already knew that ortho substitution on this part of the molecule is mandatory to get an orthogonal conformation of the aromatic ring with respect to the central core, leading to the best occupancy of the pocket without clashing with the hinge region. For this reason, all compounds shown in Table 1 have at least one ortho substituent. In this sense, compounds **8**−**11** possessing two ortho substituents were markedly more potent than the monosubstituted derivatives **4**−**7**. In particular, compound **10**, with an ortho,ortho-dichloro substitution, is the most potent one in both the enzymatic and cellular assays (p38α IC_{50} = 42 nM; LPS-induced TNFα release in THP-1 cells, IC_{50} = 14 nM).

On the other hand, based on the parent aminopyridine series,[16] we were aware of the limited solubility of these molecules, as can be exemplified by compound **4** (27 μg/mL at pH 7.4; 41 μg/mL at pH 1). Moreover, as we have learned from the previous SAR studies with the aminopyridine series,[16] the location of the hydrophobic pocket II near the solvent exposed area allows the introduction of large substituents on the para position of the R^2 aromatic ring. Therefore, we could use this position to introduce polar groups in order to increase the aqueous solubility and, potentially, to improve the PK behavior. However, as can be seen in Table 1, naphthyridines are much more sensitive than the corresponding aminopyridines toward the substitution on this position and none of the compounds tested gave an appropriate enzymatic potency or improved physicochemical properties (compounds **12**−**15**).

The postulated binding mode of these ligands (Figure 1b for putative aminopyridines) within the p38α active site suggests that not very large substituents would be tolerated in the para position of the phenyl group in R^1 because of its proximity to the back pocket of the enzyme.[22] However, ortho substitution on this group still allows a potentially interesting SAR exploration with medium size substituents. A small number of compounds (**16**−**20**) were synthesized, keeping the ortho,ortho-disubstitution pattern in R^2, and their potency in the enzymatic assay was measured (Table 2).

Compound **16** (Table 2), bearing an ortho-methoxy group, gave an enzymatic potency comparable to that of compound **11** (Table 1) but slightly inferior to that of compound **19** (Table 2). This fact showed that although a methoxy group is allowed, the size of the ortho substituents at R^1 was important. In this sense, taking into account the loss in potency in compounds **17** and **18** (Table 2), CF_3 is clearly too bulky a substituent while an ortho-chlorine atom on R^1 is allowed, matching the best pocket I occupancy with compound **20** (p38α IC_{50} = 14 nM, THP-1 cells IC_{50} = 44 nM, and TNFα in HWB IC_{50} = 360 nM).

After this preliminary exploration, compound **20** was judged as the one bearing the best substitutions on R^1 (2-Cl,4-F-Ph) and R^2 (2,6-diCl). Therefore, it was worth testing its selectivity against a panel of 55 tyrosine and serine/threonine kinases,[23] showing an impressive selectivity for p38α/β over all tested kinases (e.g., c-Raf, JNK-1−3, MK2, IC_{50} > 10 μM).

At this point, having in mind the structural motifs developed by Merck (Figure 1a), regarding the introduction of basic substituents in position 2, we contemplated the opportunity offered by our naphthyridine core.

In the case of Merck naphthyridones, quinolinones, and dihydroquinazolinones,[17,18] the introduction of a piperidinyl moiety confers aqueous solubility and increased p38α inhibition. The increased potency is presumed to arise from a salt bridge interaction between the protonated piperidine nitrogen and the carboxylate group of Asp168. Therefore, we prepared diversely substituted naphthyridines in the R^3 position (Table 3). All piperidine based substitutions in R^3 displayed excellent potencies in the enzymatic (subnanomolar range in most cases) and cellular assays. The inhibition of TNFα in a more complex system like human whole blood (hWB) was also excellent with values in the low nanomolar range (compounds **21**, **22**, and **28**).

The microsomal oxidative metabolism of these molecules was low, and following Merck's exploratory route,[17,18] we

dx.doi.org/10.1021/jm200975u|*J. Med. Chem.* 2011, 54, 7899−7910

Table 1. 4-(2,4-Difluorophenyl)-8-aryl-1,7-naphthyridine 7-Oxides: R^2 Group Exploration

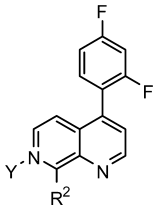

Compd.	Y	R^2	IC_{50} (nM)[a] obtained in the enzymatic and cellular assays		
			p38α	TNFα cell (THP-1)	TNFα HWB
3	-	2-Me-Ph	>1000	nd	nd
4	O	2-Me-Ph	68 (1.80)	187 (1.87)	496 (1.14)
5	O	2-OMe-Ph	144 (1.97)	nd	433 (1.12)
6	O	2-Cl-Ph	195 (1.05)	125 (1.34)	>1000
7	O	2-F-Ph	333 (1.15)	50 (1.28)	nd
8	O	2,6-diMe-Ph	148 (1.46)	144 (1.16)	255 (1.08)
9	O	2,6-diOMe-Ph	141[b]	>1000	nd
10	O	2,6-diCl-Ph	41 (1.35)	14 (1.28)	715 (2.25)
11	O	2,6-diF-Ph	66 (1.38)	190 (2.27)	257 (1.48)
12	O	4-OH-2-Me-Ph	90 (1.43)	487 (1.16)	>1000
13	O	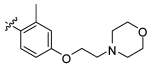	422 (1.22)	nd	>1000
14	O	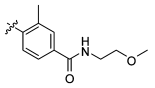	1400 (1.34)	nd	nd
15	O	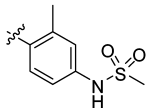	81[b]	>1000	nd

[a]Values are reported as the geometric mean of at least two independent determinations along with the geometric SD (in parentheses). nd = not determined. [b]n = 1.

decided to test the effect exerted by the substitution of the piperidine nitrogen over the potency and ADME properties. The *N*-alkyl derivatives **23**–**25** showed potencies similar to those of their unsubstituted analogues.

The introduction of basic aromatic groups (compounds **26** and **27**) or removal of the basic character by forming an acetamide (compound **29**) has a profound negative effect on the enzymatic activity, confirming the importance of the postulated salt bridge interaction with Asp168.

Following our SAR exploration over the R^3 position, we decided to study the effect of having a heteroatom as the attachment point with the naphthyridine core. For those compounds, shown in Table 4, the potency in all assays was maintained or even increased, becoming clear that the main requisite was the presence of a basic nitrogen at the appropriate position (see drop in potency for compounds **31** and **36**).

To confirm the proposed binding mode for our naphthyridine *N*-oxide scaffold **B** (Figure 2), compound **21** was cocrystallized with unphosphorylated p38α.[24] The X-ray structure (Figure 3b) revealed a binding mode compatible to

Table 2. 8-(2,6-Dichlorophenyl)-4-aryl-1,7-naphthyridine 7-Oxides: R^1 Group Optimization

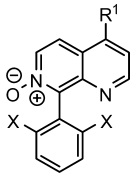

compd	X	R^1	IC_{50} (nM)[a] obtained in the enzymatic and cellular assays		
			p38α	TNFα cell (THP-1)	TNFα HWB
16	F	2-MeO-Ph	77 (1.19)	nd	292 (1.72)
17	Cl	3-CF_3-Ph	>10000	nd	nd
18	Cl	4-CF_3-Ph	>10000	nd	nd
19	Cl	2-Cl-Ph	37 (1.03)	137 (1.15)	>1000
20	Cl	2-Cl,4-F-Ph	14 (1.26)	37 (1.34)	360 (1.39)

[a]Values are reported as the geometric mean of at least two independent determinations along with the geometric SD (in parentheses). nd = not determined.

dx.doi.org/10.1021/jm200975u|J. Med. Chem. 2011, 54, 7899–7910

Table 3. 8-(2,6 -Halophenyl)-4-aryl-2-(piperidin-4-yl)-1,7-naphthyridine 7-Oxides: R^3 Group Optimization

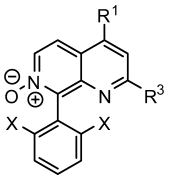

Compd.	R^1	X	R^3	IC_{50} (nM)[a] obtained in the enzymatic and cellular assays: p38α	TNFα cell(THP-1)	TNFα HWB
21	2,4-DiF-Ph	Cl	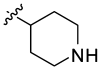	0.82 (1.98)	1.2 (2.96)	4.9 (2.25)
22	2-Cl,4-F-Ph	Cl	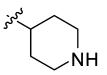	0.49 (2.20)	2.5 (2.33)	6.8 (1.39)
23	2-Cl,4-F-Ph	Cl	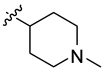	0.72 (1.67)	1.5 (1.92)	9.9 (2.09)
24	2-Cl,4-F-Ph	Cl	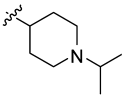	0.59 (1.09)	1.4 (1.22)	5.1 (1.73)
25	2-Cl,4-F-Ph	Cl	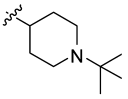	0.53 (1.48)	0.47 (1.04)	7.2 (1.08)
26	2-Cl,4-F-Ph	Cl		29 (1.11)	35 (1.38)	290 (1.99)
27	2-Cl,4-F-Ph	Cl		14 (1.14)	16 (1.24)	350 (1.15)
28	2-Cl-Ph	F	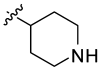	0.27 (1.12)	3.7 (1.87)	6.1 (1.89)
29	2-Cl-Ph	F	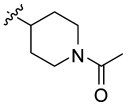	17 (1.15)	126 (1.27)	235 (2.40)

[a]Values are reported as the geometric mean of at least two independent determinations along with the geometric SD (in parentheses).

that for the previously described aminopyridines (Figure 1b), confirming that ring closure to render a naphthyridine bicyclic core was a convenient structural modification. Moreover, the X-ray structure displays a Gly flip, generating a double hydrogen bond interaction with the backbone NH of Met109 and the NH of Gly110, as in the aminopyridine series. A comparison of X-ray crystal structures of **21**[24] (Figure3b) with that of Merck inhibitor **1** (Figure 3a)[15] clearly confirmed the similarities of the key hydrogen bond interactions of both compounds with the hinge region of the enzyme. More interestingly, it was confirmed that the formation of a salt bridge with Asp168 may be responsible for the extremely high enzymatic potencies reached. Although it is true that the distance between piperidine nitrogen and the carboxylic group of Asp168 exceeded what is usually accepted for this kind of interaction, the distribution of the positive charge on the carbons adjacent to the nitrogen should account for this salt bridge being responsible of the potency boost.

The ADME profiling of some representative derivatives showed a great difference between compounds with and without a basic R^3. As shown in Table 5, compounds **21** and **30** displayed very high clearance and distribution volumes together with very low plasma levels, in contrast with the pharmacokinetic behavior shown by Merck naphthyridones, quinolinones, and dihydroquinazolinones,[17,18] with basic pendent groups. However, unsubstituted naphthyridine **4**, among the most potent compounds, showed sustained levels, low clearance ($Cl = 2.7$ mL min^{-1} kg^{-1}), and good bioavailability ($F = 38\%$). Therefore, because of its balanced potency/ADME profile, **4** was selected for further characterization.

Furthermore, compound **4** presented a low oxidative metabolic rate in rat (9%) and human (<5%) microsomes and did not inhibit any of the most relevant P450 isoforms

dx.doi.org/10.1021/jm200975u|J. Med. Chem. 2011, 54, 7899–7910

Table 4. 4-(2-Chlorophenyl)-8-(2,6-halophenyl)-2-substituted-1,7-naphthyridine 7-Oxides: R^3 Group Optimization

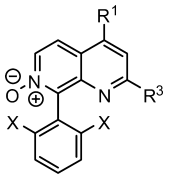

Comp	R^1	X	R^3	IC_{50} (nM)[a] obtained in the enzymatic and cellular assays: p38α	TNFα cell(THP-1)	TNFα HWB
30	2,4-diF-Ph	F	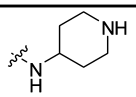	0.28 (1.25)	1.9 (1.12)	5.4 (1.44)
31	2-Cl-Ph	F		11 (1.89)	41 (1.4)	>1000
32	2-Cl-Ph	Cl	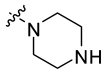	0.26 (1.65)	2 (1.04)	122 (1.82)
33	2-Cl-Ph	Cl	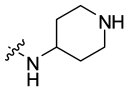	0.13 (2.02)	0.7 (1.63)	9 (1.12)
34	2-Cl-Ph	Cl	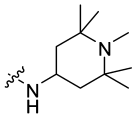	0.50 (1.16)	3.2 (1.7)	21.2 (1.11)
35	2-Cl-Ph	Cl	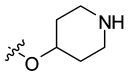	0.46 (1.61)	3.9 (2.3)	16.8 (1.13)
36	2-Cl-Ph	Cl	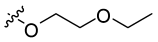	9 (1.43)	15 (1.06)	>1000

[a]Values are reported as the geometric mean of at least two independent determinations along with the geometric SD (in parentheses).

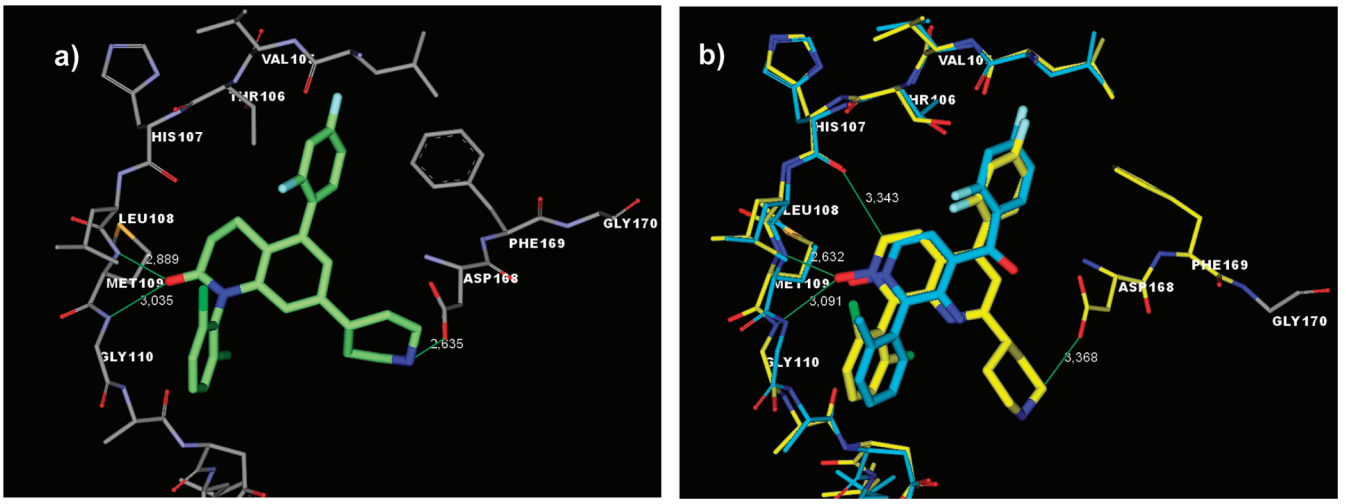

Figure 3. (a) X-ray crystal structure of Merck inhibitor **1** (shown in green, taken from the published X-ray structure).[15] (b) X-ray overlay of compounds **2** (shown in cyan)[16] and **21** (shown in yellow)[24] complexed to p38*α* active site. The conformational change of Gly110 can be seen in both proteins, revealing significant hydrogen bond interactions between Met109/Gly110 NHs and *N*-oxide oxygen in both cases. Comparing X-ray crystal structures of **21**[24] with that of Merck inhibitor **1** (Figure 1a)[15] clearly confirmed the similarities of the key hydrogen bond interactions of both compounds with the hinge region of the enzyme besides the formation of a salt bridge with Asp168.

(1A2, 3A4, 2C9, 2C19, and 2D6) at 10 μM. On the other hand, compound **4** was tested for in vitro cytotoxicity against a Chinese hamster ovary (CHO) cell line, showing a clean cytotoxic profile (30% at 200 μM).

dx.doi.org/10.1021/jm200975u|*J. Med. Chem.* 2011, 54, 7899–7910

Table 5. Pharmacokinetic Parameters of 4, 21, and 30 in Male Wistar Rat after Intravenous (iv) and Oral (po) Administration[a]

compd	dose po (mg/kg)	dose iv (mg/kg)	C_{max} po (μM)	t_{max} po (h)	AUC_{0-6} [b] po (μM h)	$t_{1/2}$ iv (h)	Cl [c] iv (mL min^{-1} kg^{-1})	V_{ss} [d] iv (L/kg)	F_{0-6} [e] (%)
4	10	1	5.3	3.5	29.5	7.4	2.7	1.7	38
21	10	1	0.2	0.3	0.48	2.3	102	13.7	16
30	10	1	0.09	0.3	0.05	4.6	59	10.3	<10

[a]Results expressed as the mean ± SD of n = 2. [b]AUC = area under the curve. [c]Cl = clearance. [d]V_{ss} = volume of distribution steady state. [e]F = bioavailability.

In Vivo Pharmacological Evaluation. To evaluate the compound's efficacy, **4** was tested in vivo in an acute model based on rat-LPS induced TNFα and in an adjuvant-induced arthritis (AIA) assay as a chronic disease model, proving to be superior to aminopyridine **2** and to standard reference compounds BIRB-796[25,26] and VX-745[11,12] (Table 6). In the rat-LPS induced TNFα model, compounds were dosed orally 1 h prior to LPS administration and the amount of TNFα in plasma was measured 1.5 h later (coinciding with the peak of TNFα production). Compound **4** dose-dependently inhibited TNFα production with an ED_{50} of 0.5 mg/kg.

Table 6. Summary of in Vivo Efficacy Assays

compd	rat LPS-induced TNF ED_{50} (mg/kg)[a]	AIA ED_{50} (mg/kg) or % inhibition[a]
4	0.5 (0.32−0.79)	<1
2	1.03 (0.5−2.07)	4.5 (1.7−11.8)
BIRB-796	7.9 (2.7−22.8)	8.6 (3.8−19.6)
VX-745	nd	>100

[a]Results represent the calculated ED_{50} along with the lower and upper 95% confidence limits (in parentheses). nd = not determined.

The adjuvant-induced arthritis (AIA) model was selected as a chronic disease model to evaluate compound efficacy (Table 6). Upon arthritis induction, compounds were administered orally once daily for 7 days. Compound **4** dose-dependently inhibited arthritis progression with ED_{50} < 1 mg/kg. These results demonstrate a superior efficacy of **4** versus other clinically tested reference compounds like BIRB-796 and VX-745, when dosed in the same manner.

CONCLUSIONS

A novel series of naphthyridine *N*-oxides were designed, synthesized, and tested for their ability to inhibit p38α MAP kinase. The proposed binding mode for this novel series of inhibitors is consistent with the crystallographic results obtained from inhibitor **21** within the p38α active site. Some of these compounds showed a significant reduction in the LPS-induced TNFα production in THP-1 cells and in hWB.

The appropriate balance between potency and pharmacokinetics of compound **4** coupled to its excellent behavior in a chronic model of arthritis highlights the potential of this compound to be further profiled in various inflammatory conditions.

EXPERIMENTAL SECTION

Chemistry. Nonaqueous reactions were performed under argon or nitrogen atmosphere at room temperature unless otherwise noted. All commercial reagents and anhydrous solvents were purchased from Aldrich and were used without further purification or distillation unless otherwise stated.

Routine ^{1}H nuclear magnetic resonance spectra were recorded on the following instruments: Varian Gemini 300 MHz, Varian Mercury plus NMR spectrometer operating at a frequency of 200 MHz, Varian Mercury plus NMR spectrometer at 400 MHz. Samples were dissolved in deuterated chloroform ($CDCl_3$) or deuterated dimethylsulfoxide (DMSO-d_6), and tetramethylsilane (TMS) was used as reference.

Analytical thin-layer chromatography (TLC) was performed on Merck silica gel 60 F_{254}. Compounds were visualized by UV light and/or stained with either potassium permanganate or cerium molybdate solutions followed by heating. Flash column chromatography was performed on SDS silica gel 60 (particle size of 40−63 μm).

HPLC analysis was performed on a Waters Alliance 2795 chromatograph equipped with a Waters 2996 diode array detector and a Waters ZQ mass spectrometer detector. HPLC analysis was conducted with the following parameters: Chromatography was performed on a Symmetry C18 column (100 mm × 2.16 mm, 3.5 μm). The mobile phase, at a flow of 0.4 mL/min, was a 20 min binary gradient of water (containing 0.01 M ammonium formate at pH 3.0) and a mixture acetonitrile−methanol 50:50 (containing 0.01 M ammonic formiate 0.01M) (0−95%). The total run time was 26 min. The retention time (t_R) is expressed in min, and UV chromatograms were processed at 210 nm with blank subtraction. All key compounds were proven by this method to show ≥95% purity.

General Procedure for the Synthesis of 1,7-Naphtyridines 3−20 (R^3 = H) (Scheme 1). 4-(2,4-Difluorophenyl)-8-(2-methylphenyl)-1,7-naphthyridine (3). To a solution of 20 mg (0.062 mmol) of **37a**[16] in 0.4 mL of glacial AcOH was added 0.3 mL of acetaldehyde, and the mixture was heated in a microwave system ("Initiator Sixty" from Biotage) at 100 °C for 45 min. The cooled mixture was poured into 50 mL of H_2O and the pH adjusted to 6−7 using 2 M NaOH. The solution was extracted with EtOAc. The organic extract was washed with brine, dried (Na_2SO_4), and evaporated. Purification by flash chromatography, eluting with hexane/EtOAc (4:1) gave 12 mg (56%) of **1**. LCMS (m/z): 333 $[M + 1]^+$. ^{1}H NMR ($CDCl_3$) δ 2.15 (s, 3H), 7.03−7.17 (m, 2H), 7.33−7.54 (m, 7H), 8.67 (d, J = 5.8 Hz, 1H), 9.04 (d, J = 4.2 Hz, 1H).

4-(2,4-Difluorophenyl)-8-(2-methylphenyl)-1,7-naphthyridine 7-Oxide (4). This compound was prepared from **37b**[16] as described in the synthesis of **3** but heating at 110 °C for 18 h. Yield: 45%. LCMS (m/z): 349 $[M + 1]^+$. ^{1}H NMR ($CDCl_3$) δ 2.18 (s, 3H), 7.03−7.18 (m, 2H), 7.30−7.54 (m, 7H), 8.33 (d, J = 8.1 Hz, 1H), 8.96 (d, J = 5.7 Hz, 1H).

4-(2,4-Difluorophenyl)-8-(2-methoxyphenyl)-1,7-naphthyridine 7-Oxide (5). This compound was prepared from **37c**[16] as described in the synthesis of **3**. Yield: 55%. LCMS (m/z): 365 $[M + 1]^+$. ^{1}H NMR ($CDCl_3$) δ 3.80 (s, 3H), 7.02−7.21 (m, 4H), 7.33−7.59 (m, 5H), 8.32 (d, J = 7.8 Hz, 1H), 8.96 (d, J = 4.1 Hz, 1H).

8-(2-Chlorophenyl)-4-(2,4-difluorophenyl)-1,7-naphthyridine 7-Oxide (6). This compound was prepared from **37d**[16] as described in the synthesis of **3**. Yield: 85%. LCMS (m/z): 369 $[M + 1]^+$. ^{1}H NMR (DMSO-d_6) δ 7.30−7.41 (m, 1H), 7.45−7.70 (m, 8H), 8.38 (d, J = 7.9 Hz, 1H), 8.94 (d, J = 4.0 Hz, 1H).

4-(2,4-Difluorophenyl)-8-(2-fluorophenyl)-1,7-naphthyridine 7-Oxide (7). This compound was prepared from **37e**[16] as described in the synthesis of **3**. Yield: 51%. LCMS (m/z): 353 $[M + 1]^+$. ^{1}H NMR (DMSO-d_6) δ 7.30−7.42 (m, 1H), 7.50−7.74 (m, 8H), 8.38 (d, J = 6.0 Hz, 1H), 8.96 (d, J = 4.0 Hz, 1H).

4-(2,4-Difluorophenyl)-8-(2,6-dimethylphenyl)-1,7-naphthyridine 7-Oxide (8). This compound was prepared from **37f**[16] as described in the synthesis of **3**. Yield: 53%. LCMS (m/z): 363 $[M + 1]^+$. ^{1}H NMR ($CDCl_3$) δ 2.03 (s, 6H), 7.04−7.17 (m, 1H), 7.11 (d, J = 7.9 Hz, 1H), 7.22−7.26 (m, 2H), 7.35 (d, J = 6.0 Hz, 1H),

dx.doi.org/10.1021/jm200975u | J. Med. Chem. 2011, 54, 7899−7910

7.38−7.47 (m, 2H), 7.53 (dd, J = 2.2, 7.9 Hz, 1H), 8.36 (d, J = 7.9 Hz, 1H), 8.96 (d, J = 6.0 Hz, 1H).

4-(2,4-Difluorophenyl)-8-(2,6-dimethoxyphenyl)-1,7-naphthyridine 7-Oxide (9). This compound was prepared from **37g**[16] as described in the synthesis of **3**. Yield: 33%. LCMS (m/z): 395 [M + 1]$^+$. ^{1}H NMR ($CDCl_3$) δ 3.74 (s, 6H), 6.76 (d, J = 7.8 Hz, 2H), 7.02−7.16 (m, 2H), 7.33 (d, J = 6.1 Hz, 1H), 7.35−7.53 (m, 2H), 7.47 (d, J = 7.9 Hz, 1H), 8.30 (d, J = 7.8 Hz, 1H), 8.94 (d, J = 6.1 Hz, 1H).

8-(2,6-Dichlorophenyl)-4-(2,4-difluorophenyl)-1,7-naphthyridine 7-Oxide (10). This compound was prepared from **37h**[16] as described in the synthesis of **3**. Yield: 57%. LCMS (m/z): 403 [M + 1]$^+$. ^{1}H NMR ($CDCl_3$) δ 7.04−7.20 (m, 2H), 7.39−7.61 (m, 6H), 8.33 (d, J = 8.2 Hz, 1H), 8.96 (d, J = 6.4 Hz, 1H).

4-(2,4-Difluorophenyl)-8-(2,6-difluorophenyl)-1,7-naphthyridine 7-Oxide (11). This compound was prepared from **37i**[16] as described in the synthesis of **3**. Yield: 71%. LCMS (m/z): 371 [M + 1]$^+$. ^{1}H NMR ($CDCl_3$) δ 7.06−7.16 (m, 4H), 7.37−7.55 (m, 3H), 7.57 (dd, J = 2.3, 6.1 Hz, 1H), 8.34 (d, J = 8.0 Hz, 1H), 8.97 (d, J = 6.1 Hz, 1H).

4-[4-(2,4-Difluorophenyl)-7-oxido-1,7-naphthyridin-8-yl]-3-methylphenol (12). This compound was prepared from **37j**[16] as described in the synthesis of **3**. Yield: 32%. LCMS (m/z): 365 [M + 1]$^+$. ^{1}H NMR ($CDCl_3$) δ 2.09 (s, 3H), 6.64−6.69 (m, 2H), 7.04−7.16 (m, 3H), 7.38−7.44 (m, 2H), 7.54 (dd, J = 1.7, 8.0 Hz, 1H), 8.37 (d, J = 6.2 Hz, 1H), 9.02 (d, J = 4.1 Hz, 1H).

4-(2,4-Difluorophenyl)-8-[2-methyl-4-(2-morpholin-4-ylethoxy)phenyl]-l,7-naphthyridine 7-Oxide (13). This compound was prepared from **37k**[16] as described in the synthesis of **3** but heating at 110 °C for 18 h. Yield: 14%. LCMS (m/z): 478 [M + 1]$^+$.

4-[4-(2,4-Difluorophenyl)-7-oxido-1,7-naphthyridin-8-yl]-*N*-(2-methoxyethyl)-3-methyl-benzamide (14). This compound was prepared from **37l**[16] as described in the synthesis of **3** but heating at 110 °C for 18 h Yield: 23%. LCMS (m/z): 450 [M + 1]$^+$.

***N*-{4-[4-(2,4-Difluorophenyl)-7-oxido-1,7-naphthyridin-8-yl]-3-methylphenyl}methanesulfonamide (15).** This compound was prepared from **37m**[16] as described in the synthesis of **3**. Yield: 21%. LCMS (m/z): 442 [M + 1]$^+$. ^{1}H NMR ($CDCl_3$) δ 2.15 (s, 3H), 3.08 (s, 3H), 7.04−7.23 (m, 5H), 7.39−7.45 (m, 2H), 7.57 (dd, J = 2.3, 6.1 Hz, 1H), 8.00 (brs, 1H), 8.37 (d, J = 7.8 Hz, 1H), 8.99 (d, J = 6.1 Hz, 1H).

8-(2,6-Difluoropheny1)-4-(2-methoxypheny1)-1,7-naphthyridine 7-Oxide (16). This compound was prepared from **37n**[16] as described in the synthesis of **3**. Yield: 45%. LCMS (m/z): 365 [M + 1]$^+$. ^{1}H NMR ($CDCl_3$) δ 3.78 (s, 3H), 7.08−7.18 (m, 4H), 7.27−7.31 (m, 1H), 7.37 (d, J = 4 Hz, 1H), 7.47−7.60 (m, 3H), 8.27 (d, J = 6 Hz, 1H), 8.94 (d, J = 4 Hz, 1H).

8-(2,6-Dichlorophenyl)-4-[3-(trifluoromethyl)phenyl]-1,7-naphthyridine 7-Oxide (17). This compound was prepared from **37o**[16] as described in the synthesis of **3**. Yield: 57%. LCMS (m/z): 435 [M + 1]$^+$. ^{1}H NMR ($CDCl_3$) δ 7.42 (d, J = 6.3 Hz, 1H), 7.44−7.57 (m, 3H), 7.73−7.76 (m, 2H), 7.74 (d, J = 8.0 Hz, 1H), 7.80−7.88 (m, 2H), 8.34 (d, J = 8.0 Hz, 1H), 8.97 (d, J = 6.3 Hz, 1H).

8-(2,6-Dichlorophenyl)-4-[4-(trifluoromethyl)phenyl]-1,7-naphthyridine 7-Oxide (18). This compound was prepared from **37m**[16] as described in the synthesis of **3**. Yield: 64%. LCMS (m/z): 435 [M + 1]$^+$. ^{1}H NMR ($CDCl_3$) δ 7.41 (d, J = 5.7 Hz, 1H), 7.46−7.57 (m, 3H), 7.68 (d, J = 7.9 Hz, 2H), 7.75 (d, J = 7.9 Hz, 1H), 7.88 (d, J = 8.0 Hz, 2H), 8.34 (d, J = 7.9 Hz, 1H), 8.97 (d, J = 3.6 Hz, 1H).

4-(2-Chlorophenyl)-8-(2,6-dichlorophenyl)-1,7-naphthyridine 7-Oxide (19). This compound was prepared from **37n**[16] as described in the synthesis of **3**. Yield: 13%. LCMS (m/z): 401 [M + 1]$^+$. ^{1}H NMR ($CDCl_3$) δ 7.33−7.58 (m, 8H), 7.59−7.68 (m, 1H), 8.29 (d, J = 7.4 Hz, 1H), 8.97 (d, J = 4.4 Hz, 1H).

4-(2-Chloro-4-fluorophenyl)-8-(2,6-dichlorophenyl)-1,7-naphthyridine 7-Oxide (20). This compound was prepared from **37o**[16] as described in the synthesis of **3**. Yield: 16%. LCMS (m/z): 419 [M + 1]$^+$. ^{1}H NMR ($CDCl_3$) δ 7.27−7.57 (m, 8H), 8.30 (d, J = 5.6 Hz, 1H), 8.98 (d, J = 4.0 Hz, 1H).

General Procedure for the Synthesis of 1,7-Naphtyridines 21, 22, 25−28 (Scheme 1). 8-(2,6-Dichlorophenyl)-4-(2,4-difluorophenyl)-2-(piperidin-4-yl)-l,7-naphthyridine 7-Oxide (21). An amount of 0.2 mL (3.85 mmol) of H_2SO_4 98% was added dropwise to a suspension of 200 mg (0.506 mmol) of **37p**,[16] 400 mg (3.7 mmol) of anhydrous $MgSO_4$, and 252 mg (1.11 mmol) of *tert*-butyl 4-acetylpiperidine-1-carboxylate in 6 mL of toluene, and the mixture was vigorously stirred in a preheated oil bath at 115 °C. After 60 min, the mixture was cooled and the solvent discarded. The residue was washed with EtOAc, dissolved in MeOH, and filtered through a sintered glass to eliminate most of the inorganic salts. Evaporation and purification by reverse phase chromatography, eluting with H_2O/ACN (0.1% of HCOOH) (from 0% to 50% of ACN), gave 180 mg. Yield: 73%. LCMS (m/z): 486 [M + 1]$^+$. ^{1}H NMR ($CDCl_3$) δ 1.55−1.94 (m, 4H), 2.64−2.77 (m, 2H), 2.84−3.00 (m, 1H), 3.08−3.20 (m, 2H), 7.02−7.16 (m, 2H), 7.29−7.55 (m, 6H), 8.28 (d, J = 8 Hz, 1H).

4-(2-Chloro-4-fluorophenyl)-8-(2,6-dichlorophenyl)-2-piperidin-4-yl-1,7-naphthyridine 7-Oxide (22). This compound was prepared from **37q**[16] as described in the synthesis of **3**. Yield: 36%. LCMS (m/z): 502 [M + 1]$^+$. ^{1}H NMR ($CDCl_3$) δ 2.04−2.10 (m, 2H), 2.25−2.36 (m, 2H), 3.00−3.10 (m, 2H), 3.19 (m, 1H), 3.28−3.34 (m, 2H), 7.16−7.26 (m, 2H), 7.35−7.54 (m, 6H), 8.28 (d, J = 7.7 Hz, 1H).

2-(1-*tert*-Butylpiperidin-4-yl)-4-(2-chloro-4-fluorophenyl)-8-(2,6-dichlorophenyl)-1,7-naphthyridine 7-Oxide (25). This compound was prepared from **37r**[16] as described in the synthesis of **3**. Yield: 32%. LCMS (m/z): 558 [M + 1]$^+$. ^{1}H NMR ($CDCl_3$) δ 1.08 (s, 9H), 1.75−1.81 (m, 2H), 1.93−1.96 (m, 2H), 2.17−2.23 (m, 2H), 2.78 (m, 1H), 3.06−3.10 (m, 2H), 7.21 (m, 1H), 7.29 (s, 1H), 7.36−7.45 (m, 4H), 7.49−7.53 (m, 2H), 8.25 (d, J = 9.2 Hz, 1H).

4-(2-Chlorophenyl)-8-(2,6-dichlorophenyl)-2-pyridin-4-yl-1,7-naphthyridine 7-Oxide (26). This compound was prepared from **37s**[16] as described in the synthesis of **3**. Yield: 51%. LCMS (m/z): 496 [M + 1]$^+$. ^{1}H NMR ($CDCl_3$) δ 7.19−7.32 (m, 1H), 7.38−7.53 (m, 4H), 7.54−7.62 (m, 2H), 7.79 (d, J = 6.0 Hz, 2H), 7.86 (s, 1H), 8.31 (d, J = 7.4 Hz, 1H), 8.71 (d, J = 6.0 Hz, 2H).

4-(2-Chloro-4-fluorophenyl)-8-(2,6-dichlorophenyl)-2-pyridin-3-yl-1,7-naphthyridine 7-Oxide (27). This compound was prepared from **37t**[16] as described in the synthesis of **3**. Yield: 50%. LCMS (m/z): 496 [M + 1]$^+$. ^{1}H NMR ($CDCl_3$) δ 7.20−7.29 (m, 2H), 7.32−7.59 (m, 6H), 7.84 (s, 1H), 8.20 (d, J = 8.0 Hz, 1H), 8.29 (d, J = 7.4 Hz, 1H), 8.67 (d, J = 4.9 Hz, 1H), 9.19 (s, 1H).

4-(2-Chlorophenyl)-8-(2,6-difluorophenyl)-2-piperidin-4-yl-1,7-naphthyridine 7-Oxide (28). This compound was prepared from **37u**[16] as described in the synthesis of **3**. Yield: 50%. LCMS (m/z): 452 [M + 1]$^+$. ^{1}H NMR ($CDCl_3$) δ 1.62−1.89 (m, 2H), 1.99 (dd, J = 13.7, 3.5 Hz, 2H), 2.70−2.88 (m, 2H), 2.88−3.10 (m, 1H), 3.12−3.29 (m, 2H), 7.04−7.19 (m, 2H), 7.27 (s, 2H), 7.32−7.65 (m, 6H), 8.26 (d, J = 7.0 Hz, 1H).

Synthesis of 4-(2-Chloro-4-fluorophenyl)-8-(2,6-dichlorophenyl)-2-(1-methylpiperidin-4-yl)-1,7-naphthyridine 7-Oxide (23) (Scheme 2). 0.017 mL (0.47 mmol) of formic acid and 0.034 mL (0.47 mmol) of formaldehyde (37% in water) were added to 34 mg (0.06 mmol) of **22**, and the mixture was heated at 80 °C for 4 h and at room temperature for 16 h. Purification by reverse phase chromatography, eluting with H_2O/ACN (0.1% of HCOOH) (from 0% to 50% of ACN) gave 5.4 mg (17%). LCMS (m/z): 516 [M + 1]$^+$. ^{1}H NMR ($CDCl_3$) δ 1.76−1.87 (m, 4H), 2.00−2.08 (m, 2H), 2.27 (s, 3H), 2.76−2.80 (m, 1H), 2.80−2.93 (m, 2H), 7.05−7.11 (m, 2H), 7.38−7.52 (m, 5H), 7.55−7.60 (m, 1H), 8.24 (d, J = 4.2 Hz, 1H).

Synthesis of 4-(2-Chloro-4-fluorophenyl)-8-(2,6-dichlorophenyl)-2-(1-isopropylpiperidin-4-yl)-1,7-naphthyridine 7-Oxide (24) (Scheme 2). 127 mg (1.04 mmol) of 2-bromopropane, 8.63 mg (0.05 mmol) of potassium iodide, and 71 mg (0.52 mmol) of potassium carbonate were sequentially added to a solution of 131 mg (0.26 mmol) of **22** in 2.6 mL of acetonitrile, and the mixture was stirred at 80 °C for 7 h. After cooling, the reaction mixture was filtered through a sintered glass to eliminate most of the inorganic salts. Evaporation and purification by reverse phase chromatography, eluting with H_2O/ACN (0.1% of HCOOH) (from 0% to 50% of ACN), gave 89 mg (67%). LCMS (m/z): 544 [M + 1]$^+$. ^{1}H NMR ($CDCl_3$) δ 1.05 (d, J = 5.8 Hz, 6H), 1.73−1.83 (m, 2H), 1.93−1.96 (m, 2H), 2.22−2.27 (m, 2H), 2.69−2.75 (m 1H), 2.76−2.83 (m, 1H), 2.91−2.94 (m, 2H),

dx.doi.org/10.1021/jm200975u | J. Med. Chem. 2011, 54, 7899−7910

7.17−7.22 (m, 1H), 7.27 (s, 1H), 7.35−7.44 (m, 4H), 7.48−7.51 (m, 2H), 8.25 (d, J = 8.0 Hz, 1H).

Synthesis of 2-(1-Acetylpiperidin-4-yl)-4-(2-chlorophenyl)-8-(2,6-difluorophenyl)-1,7-naphthyridine 7-Oxide (29) (Scheme 2). To a solution of 50 mg (0.15 mmol) of **28** in 1.5 mL of CH_2Cl_2 were added 0.035 mL (0.25 mmol) of Et_3N and 0.014 mL (0.20 mmol) of acetyl chloride. The mixture was stirred under argon at room temperature for 48 h. The reaction mixture was quenched by the addition of 1 mL of H_2O and stirred at room temperature for 10 min. Then it was diluted with EtOAc, washed with 2 N HCl, brine, dried, and evaporated. Purification by reverse phase chromatography, eluting with H_2O/ACN (0.1% of HCOOH) (from 0% to 70% of ACN), gave 50 mg (65%). LCMS (m/z): 494 $[M + 1]^+$. ^{1}H NMR ($CDCl_3$) δ 1.66−1.83 (m, 2H), 1.99 (dd, J = 10.9, 5.1 Hz, 2H), 2.10 (s, 3H), 2.69−2.88 (m, 1H), 2.98−3.11 (m, 1H), 3.14−3.26 (m, 1H), 3.85 (d, J = 14.8 Hz, 1H), 4.44−4.64 (m, 1H), 7.03−7.17 (m, 2H), 7.31−7.66 (m, 7H), 8.27 (d, J = 7.1 Hz, 1H).

General Procedure for the Synthesis of 1,7-Naphtyridines 30−36 ($R^3 \neq H$) (Scheme 3). 4-(2,4-Difluorophenyl)-8-(2,6-difluorophenyl)-l,7-naphthyridin-2(1*H*)-one (39a). (a) To a solution of **38a**[16] (1.5 g, 4 mmol) and diisopropylethylamine (1.5 mL, 8.6 mmol) in 10 mL of dioxane under argon was carefully added pivaloyl chloride (1 mL, 8.1 mmol) in 5 mL of dioxane. After the addition was completed, the reaction mixture was stirred at 110 °C for 18 h. The mixture was diluted with EtOAc, washed with water, aqueous 4% sodium bicarbonate, brine, dried over sodium sulfate and the solvent removed under reduced pressure. The residue obtained was triturated with pentane to afford a solid that was filtered to yield 1.58 g (88%) of *N*-[4-(2,4-difluorobenzoyl)-2-(2,6-difluorophenyl)-pyridin-3-yl]-2,2-dimethylpropanamide. LCMS (m/z): 431 $[M + 1]^+$.

(b) Subsequently, *n*-BuLi (1.6 M in hexanes, 8.8 mL, 14.1 mmol) was added dropwise to a solution of diisopropylamine (2 mL, 14.2 mmol) in dry tetrahydrofuran (10 mL) at −78 °C under argon, and the resulting mixture was stirred at room temperature for 20 min. Then the reaction mixture was cooled to −78 °C and *tert*-butyl acetate (1.9 g, 14.1 mmol) in dry tetrahydrofuran (5 mL) was added. Afterward, the compound obtained in the previous step (1.6 g, 3.52 mmol) in dry tetrahydrofuran (10 mL) was added and the mixture stirred overnight at room temperature. Subsequently, the solvent was removed under reduced pressure and the residue was partitioned between EtOAc (80 mL) and water (80 mL). The organic solution was washed with brine, dried over anhydrous sodium sulfate and the solvent removed under reduced pressure to yield 3-(2,4-difluorophenyI)-3-[2-(2,6-difluorophenyl)-3-(2,2-dimethylpropiony1amino)-pyridin-4-yl]-3-hydroxypropionic acid *tert*-butyl ester (1.9 g, 99%) as a pale yellow solid. LCMS (m/z): 547 $[M + 1]^+$.

(c) In the next step, a mixture of the previous intermediate (1.9 g, 3.52 mmol) and 5 M aqueous solution of HCl (30 mL) was stirred at 100 °C overnight. The mixture was carefully neutralized with a saturated solution of potassium carbonate in water, and the precipitated solid was filtered to yield the title compound (1.2 g, 88%) as a solid. LCMS (m/z): 371 $[M + 1]^+$. ^{1}H NMR ($CDCl_3$) δ 6.78 (s, 1H), 7.11 (d, J = 5.3 Hz, 1H), 7.25−7.62 (m, 6H), 8.48 (d, J = 5.3 Hz, 1H), 8.55 (bs, 1H).

4-(2-Chlorophenyl)-8-(2,6-difluorophenyl)-l,7-naphthyridin-2(1*H*)-one (39b). This compound was prepared from **38b**[14] following the experimental procedure described for the synthesis of **39a**. Yield: 60% (over the three steps). LCMS (m/z): 370 $[M + 1]^+$. ^{1}H NMR (300 MHz, $CDCl_3$) δ 6.78 (s, 1H), 7.20−7.04 (m, 3H), 7.36 (m, 1H), 7.52 (m, 4H), 8.48 (d, J = 5.3 Hz, 1H), 8.56 (bs, 1H).

4-(2-Chlorophenyl)-8-(2,6-dichlorophenyl)-l,7-naphthyridin-2(1*H*)-one (39c). This compound was prepared from **38c**[14] following the experimental procedure described for the synthesis of **39a**. Yield: 50% (over the three steps). LCMS (m/z): 401 $[M + 1]^+$. ^{1}H NMR (300 MHz, $CDCl_3$) δ 6.78 (bd, J = 1.6 Hz, 1H), 7.11 (d, J = 5.3 Hz, 1H), 7.65−7.34 (m, 7H), 8.39 (bs, 1H), 8.48 (d, J = 5.3 Hz, 1H).

4-(2,4-Difluorophenyl)-8-(2,6-difluorophenyl)-l,7-naphthyridin-2(1*H*)-one 7-Oxide (40a). A mixture of intermediate **39a** (0.3 g, 0.81 mmol), acetic acid (8 mL), and 30% hydrogen peroxide (2 mL) was heated at 95 °C in a sealed tube for 16 h. The reaction mixture was diluted with water (50 mL) and extracted with EtOAc (3 × 40 mL). The organic layer was dried over sodium sulfate and the solvent removed under reduced pressure to yield the title compound (0.27 g, 85%) as a solid. LCMS (m/z): 387 $[M + 1]^+$. ^{1}H NMR (300 MHz, DMSO-d_6) δ 6.64 (s, 1H), 7.43−7.12 (m, 5H), 7.80−7.45 (m, 3H), 8.17 (d, J = 6.7 Hz, 1H).

4-(2-Chlorophenyl)-8-(2,6-difluorophenyl)-l,7-naphthyridin-2(1*H*)-one 7-Oxide (40b). This compound was prepared from **39b** following the experimental procedure described for the synthesis of **40a**. Yield: 98%. LCMS (m/z): 385 $[M + 1]^+$. ^{1}H NMR (300 MHz, $CDCl_3$) δ 6.56 (bd, J = 1.6 Hz, 1H) 7.71−6.93 (m, 8H), 8.18−7.99 (m, 1H), 8.89 (bs, 1H).

4-(2-Chlorophenyl)-8-(2,6-dichlorophenyl)-l,7-naphthyridin-2(1*H*)-one 7-Oxide (40c). This compound was prepared from **39c** following the experimental procedure described for the synthesis of **40a**. Yield: 91%. LCMS (m/z): 417 $[M + 1]^+$. ^{1}H NMR (300 MHz, $CDCl_3$) δ 6.57 (s, 1H), 7.07 (d, J = 7.1 Hz, 1H), 7.69−7.32 (m, 7H), 8.07 (d, J = 7.0 Hz, 1H), 8.27 (bs, 1H).

2-Chloro-4-(2,4-difluorophenyl)-8-(2,6-difluorophenyl)-l,7-naphthyridine 7-Oxide (41a). A mixture of the intermediate compound **40a** (0.361 g, 0.9 mmol) and phosphorus oxychloride (5 mL) was heated at 110 °C in a sealed tube for 2 h. The mixture was cooled, poured into ice−water and the pH adjusted to 10−11 with concentrated aqueous ammonia. The solution was extracted with EtOAc (2 × 100 mL), the organic layer was washed with brine, dried over sodium sulfate, and the solvent removed under reduced pressure. The residue was crystallized with isopropanol to yield compound **41a** (0.34 g, 78%) as a yellow solid. LCMS (m/z): 405 $[M + 1]^+$. ^{1}H NMR (300 MHz, DMSO-d_6) δ 7.46−7.25 (m, 2H), 7.80−7.53 (m, 5H), 7.81 (s, 1H), 8.49 (d, J = 7.4 Hz, 1H).

2-Chloro-4-(2-chlorophenyl)-8-(2,6-difluorophenyl)-l,7-naphthyridine 7-Oxide (41b). This compound was prepared from **40b** following the experimental procedure described for the synthesis of **41a**. Yield: 55%. LCMS (m/z): 403 $[M + 1]^+$. ^{1}H NMR (300 MHz, $CDCl_3$) δ 7.11 (m, 2H), 7.41−7.29 (m, 3H), 7.67−7.42 (m, 4H), 8.28 (d, J = 7.4 Hz, 1H).

2-Chloro-4-(2-chlorophenyl)-8-(2,6-dichlorophenyl)-l,7-naphthyridine 7-Oxide (41c). This compound was prepared from **40c** following the experimental procedure described for the synthesis of **41a**. Yield: 68%. LCMS (m/z): 435 $[M + 1]^+$. ^{1}H NMR (300 MHz, $CDCl_3$) δ 7.10 (m, 2H), 7.25−7.38 (m, 3H), 7.39−7.60 (m, 4H), 8.20 (d, J = 7.4 Hz, 1H).

4-(2,4-Difluorophenyl)-8-(2,6-difluorophenyl)-*N*-piperidin-4-yl-l,7-naphthyridin-2-amine 7-Oxide (30). (a) A mixture of compound **41a** (179 mg, 0.40 mmol) and *tert*-butyl 4-amino-piperidine-1-carboxylate (188 mg, 0.9 mmol) in ethoxyethanol (2 mL) was heated at 130 °C in a sealed tube for 3 h. The mixture was cooled, diluted with EtOAc (40 mL), washed with water, brine, and dried over sodium sulfate, and the solvent was removed under reduced pressure. The residue was purified by column chromatography on silica gel, eluting with hexane/EtOAc, 1/4, to yield intermediate 4-[8-(2,6-difluorophenyl)-4-(2,4-difluorophenyl)-7-oxy-l,7-naphthyridin-2-ylamino]piperidine-1-carboxylic acid *tert*-butyl ester (100 mg, 46%) as a solid. LCMS (m/z): 569 $[M + 1]^+$.

(b) A mixture of the previous intermediate compound (100 mg, 0.17 mmol) and a solution of hydrochloric acid in dioxane (4M, 3 mL) was stirred for 90 min at room temperature. The solvent was removed under reduced pressure, and the residue was partitioned between EtOAc (30 mL) and a saturated solution of sodium bicarbonate (30 mL). The organic solution was washed with brine, dried over anhydrous sodium sulfate and the solvent removed under reduced pressure to yield the title compound (60 mg, 74%) as a solid. LCMS (m/z): 469 $[M + 1]^+$. ^{1}H NMR (CD_3OD) δ 1.36−1.43 (m, 2H), 1.92−1.99 (m, 2H), 2.1 5 (s, 1H), 2.42−2.53, (m, 2H), 2.99−3.06 (m, 2H), 3.57−3.66 (m, 1H), 6.81 (s, 1H), 7.12−7.23 (m, 4H), 7.47−7.64 (m, 3H), 8.09 (d, J = 6.6 Hz, 1H).

4-(2-Chlorophenyl)-8-(2,6-difluorophenyl)-2-morpholino-l,7-naphthyridin-2-amine 7-Oxide (31). **31** was obtained as a white solid (70 mg, 35% yield) from intermediate compound **41b** (177 mg) following the experimental procedure described for the synthesis of **30a**. LCMS (m/z): 454 $[M + 1]^+$. ^{1}H NMR ($CDCl_3$) δ: 3.47−3.63

dx.doi.org/10.1021/jm200975u | J. Med. Chem. 2011, 54, 7899−7910

(m, 4H), 3.69−3.80 (m, 4H), 6.84 (s, 1H), 7.01−7.11 (m, 2H), 7.14 (d, 1H), 7.31−7.37 (m, 1H), 7.39−7.51 (m, 3H), 7.55−7.63 (m, 1H), 8.06 (d, 1H).

4-(2-Chlorophenyl)-8-(2,6-dichlorophenyl)-2-piperazin-l-yl-l,7-naphthyridine 7-Oxide (32). **32** was obtained as a white solid (52% yield) from intermediate compound **41c** following the experimental procedure described for the synthesis of **30**. LCMS (m/z): 485 $[M + 1]^+$. ^{1}H NMR ($CDCl_3$) δ: 2.83−2.92 (m, 4H), 3.46−3.55 (m, 4H), 6.85 (s, 1H), 7.14 (d, 1H), 7.32−7.42 (m, 2H), 7.42−7.52 (m, 4H), 7.55−7.62 (m, 1H), 8.02 (d, 1H).

4-(2-Chlorophenyl)-8-(2,6-dichlorophenyl)-*N*-piperidin-4-yl-l,7-naphthyridin-2-amine 7-Oxide (33). **33** was obtained as a white solid (68%) from intermediate compound **41c** following the experimental procedure described for the synthesis of **30**. LCMS (m/z): 499 $[M + 1]^+$. ^{1}H NMR ($CDCl_3$) δ 1.12−1.38 (m, 3H), 1.93−1.97 (m, 2H), 2.32−2.54 (m, 2H), 2.92−3.09 (m, 2H), 3.44−3.63 (m, 1H), 4.80 (bd, J = 6.6 Hz, 1H), 6.48 (s, 1H), 7.12 (d, J = 7.1 Hz, 1H), 7.31−7.50 (m, 6H), 7.52−7.62 (m, 1H), 8.02 (d, J = 7.1 Hz, 1H).

4-(2-Chlorophenyl)-8-(2,6-dichlorophenyl)-*N*-(l,2,2,6,6-pentamethylpiperidin-4-yl)-1,7-naphthyridin-2-amine 7-Oxide (34). **34** was obtained as a white solid (6%) from intermediate compound **41c** following the experimental procedure described for the synthesis of **30a**. LCMS (m/z): 569 $[M + 1]^+$. ^{1}H NMR ($CDCl_3$) δ 1.10 (s, 6H), 1.14−1.32 (m, 2H), 1.46 (s, 6H), 1.83 (m, 3H), 2.20 (s, 3H), 4.11 (m, 1H), 4.59 (bd, J = 7.9 Hz, 1H), 6.45 (s, 1H), 7.11 (d, J = 7.1 Hz, 1H), 7.27−7.51 (m, 6H), 7.52−7.63 (m, 1H), 8.02 (d, J = 7.1 Hz, 1H).

4-(2-Chlorophenyl)-8-(2,6-dichlorophenyl)-2-(piperidin-4-yloxy)-l,7-naphthyridine 7-Oxide (35). **35** was obtained as a white solid (31%) from intermediate compound **41c** following the experimental procedure described for the synthesis of **30a**. LCMS (m/z): 500 $[M + 1]^+$. ^{1}H NMR ($CDCl_3$) δ 1.48−1.67 (m, 2H), 1.96 (m, 2H), 2.52 (m, 2H), 3.06 (m, 2H), 3.70 (s, 1H), 4.63−4.81 (m, 1H), 6.83 (s, 1H), 7.28 (d, J = 7.2 Hz, 1H), 7.45 (m, 6H), 7.59 (m, 1H), 8.17 (d, J = 7.2 Hz, 1H).

4-(2-Chlorophenyl)-8-(2,6-dichlorophenyl)-2-(2-ethoxyethoxy)-1,7-naphthyridine 7-Oxide (36). **36** was obtained as a white solid (82%) from intermediate compound **41c** following the experimental procedure described for the synthesis of **30a**. LCMS (m/z): 489 $[M + 1]^+$. ^{1}H NMR ($CDCl_3$) δ 1.20 (m, 3H), 3.42−3.56 (m, 2H), 3.65 (m, 2H), 4.18−4.35 (m, 2H), 6.92 (s, 1H), 7.22−7.32 (m, 1H), 7.33−7.54 (m, 6H), 7.54−7.64 (m, 1H), 8.18 (d, J = 7.2 Hz, 1H).

Biological Methods. p38α Kinase Inhibition Assay. Enzymatic activity assay was performed in 96-well microtiter plates (Corning, catalog number 3686) using a total volume of 50 μL of an assay buffer composed of 50 mM HEPES, pH 7.5, 10 mM $MgCl_2$, 1.75 mM Na_3VO_4.

Various concentrations of the test compound or vehicle controls were preincubated for 1 h with 0.055 μg/mL of the human p38α (SAPKa) enzyme (obtained from University of Dundee, U.K.). The reaction started by addition of biotinylated ATF2 substrate and ATP in concentrations around their K_m values (final concentration 0.62 and 60 μM, respectively) and took place for 1 h at 25 °C. Addition of the detection reagents, streptavidin−XL665 and anti-phospho residue antibody coupled to europium cryptate, caused the juxtaposition of the cryptate and the XL665 fluorophore, resulting in fluorescence energy transfer (FRET). The FRET intensity depends on the amount of bounded cryptate antibody, which is proportional to the extent of substrate phosphorylation. FRET intensity was measured using Victor 2V spectrofluorometer.

Data were analyzed by nonlinear regression (Hill equation) to generate a dose−response curve. The calculated IC_{50} is the concentration of the test compound that caused a 50% decrease in the maximal FRET intensity.

Inhibition of TNFα Production Induced by LPS in the Human Monocytic Cell Line THP-1 Assay. For this purpose, 2 × 10^5 cells/well were plated in tissue-culture-treated round-bottom 96-well plates in RPMI (containing 10% FCS, 2mM L-Gln, 10 mM Hepes buffer, 1 mM sodium pyruvate, 4.5 g/L glucose, 1.5 g/L $NaHCO_3$, and β-mercaptoethanol 50 μM), together with compounds at the desired test concentration and LPS (Sigma, L2630) at a final concentration of 10 μg/mL. Compounds were resuspended in 100% DMSO at 1 mM and titrated thereof in 10× dilutions in medium. Controls included unstimulated and stimulated cells treated with the highest concentration of compound vehicle (1% DMSO). Cells were incubated for 5 h at 37 °C in a 5% CO_2 atmosphere. Cell supernatant was recovered by centrifugation and diluted 5-fold prior to testing in a standard human TNFα ELISA (RnD systems).

Inhibition of TNFα Production Induced by LPS in Human Whole Blood assay. Healthy volunteer donor blood was collected by venipuncture in heparinized tubes. An amount of 2 μL of 10-fold compound concentrations in 100% DMSO was mixed with 200 μL of LPS-stimulated blood in microtiter plates. Controls included unstimulated and stimulated blood treated with the highest concentration of compound vehicle (1% DMSO). Plates were incubated for 24 h at 37 °C with shaking. Supernatant was recovered by centrifugation and diluted 1 in 6 prior to testing in a standard TNFα ELISA (RnD systems).

Data were analyzed by nonlinear regression (Hill equation) to generate a dose−response curve. The calculated IC_{50} value corresponds to the concentration of the test compound causing a 50% decrease in the maximal TNFα production (absolute IC_{50}).

In Vivo Assays. LPS-Induced TNFα in the Rat. One hour prior to LPS administration, rats were dosed orally with the compounds suspended in 0.5% methylcellulose/0.1% Tween-80. LPS (5 mg/kg) was administered intraperitoneally, and 1.5 h later, rats were anesthesized and retroorbital blood was collected in heparin tubes. Plasma was separated by centrifugation and diluted one-fifth prior to assaying in a standard rat TNF-α ELISA (RnD Systems).

Adjuvant-Induced Arthritis (AIA) Model. Arthritis was induced by intraplantar administration of 100 μL of *Mycobacterium tuberculosis* suspension (5 mg/mL in paraffin oil) in the left paw of male Wistar rats (day 0). On day 11 after inoculation, animals were weighed and paw volume was measured by plesthimometry. Animals with left paw volumes ranging between 3.5 and 5 mL and right paw volumes between 2 and 3 mL were randomized in the required treatment groups (7 animals/group). Treatment was started and continued for 7 consecutive days. On each day animals were weighed and appropriately dosed orally with the indicated doses of compounds suspended in 0.5% methylcellulose/0.1% Tween 80. Paw volumes were monitored every other day. A healthy control group was inoculated with paraffin oil on day 0 and monitored thereafter for paw volumes and weight. At the end of the study, animals were euthanized with CO_2. Inhibition percentage was calculated using last day contralateral (right) paw volumes.

ADME Methods. In Vitro Studies. Metabolic Stability. Metabolic stability of test compounds was evaluated in rat and human liver microsomes. Test compounds (5 μM) were incubated in liver microsomes (1 mg/mL protein) at 37 °C for 30 min in the presence and absence of NADPH (cofactor). Test compounds from the incubations were analyzed using UPLC−MS/MS. The metabolic rate was calculated by comparison of the area of the parent compound in the incubations in the presence and absence of NADPH.

CYP Inhibition. The potential to inhibit CYP1A2, 2C9, 2C19, 2C6, and 3A4 was evaluated in human microsomes in the presence of the appropriate substrates (1A2, ethoxyresorufin; 2C9, diclofenac; 2C19, S-mephenytoin;. 2D6, dextromethorphan; 3A4, testosterone). Human liver microsomes (0.1 mg/mL protein for all isoforms with the exception of 2C19 (0.5 mg/mL protein)) were incubated at 37 °C for 10 min (1A2, 2C9, and 3A4), 30 min (2D6), or 60 min (2C19) with various concentrations of test compounds (0, 1, 5, and 25 μM) in the presence of an NADPH-generated system. To determine the activity, the amount of metabolite formed for each substrate was quantified by UPLC−MS/MS at the different concentrations of the tested compounds.

In Vivo Studies. PK Studies in Rats. Test compounds were administered to Wistar rats (1 mg/kg iv, 10 mg/kg po). Blood samples were drawn from the retro-orbital plexus at specific time points. After centrifugation (3000 rpm, 10 min, 4 °C), plasma was separated and stored at −20 °C until analysis. Samples were prepared by protein

precipitation followed by UPLC−MS/MS analysis. PK parameters were calculated using WinNolin.

■ ASSOCIATED CONTENT

Supporting Information

Kinase selectivity panel for compound **20**. This material is available free of charge via the Internet at http://pubs.acs.org.

Accession Codes

†Coordinates and structure factors have been deposited in the RCSB Protein Data Bank (access code 3MW1 for complex of p38α with **21**).

■ AUTHOR INFORMATION

Corresponding Author

*Phone: 34 93 291 35 83. Fax: 34 93 291 34 20. E-mail: juan.francisco.caturla@almirall.com.

Present Address

#Eli Lilly & Co. Centro de Investigación Lilly, S.A. Avda. de la Industria, 30, 28108 Alcobendas (Madrid), Spain.

■ ACKNOWLEDGMENTS

We thank Josep Maria Huerta for spectroscopic data and Ramón Roca for molecular modeling. We gratefully acknowledge Phil Leonard, Marieke Lamers, and Martin Fisher from BioFocus DPI (formerly at Sareum) for their kind assistance in the crystallographic studies of compound **21**.

■ ABBREVIATIONS USED

MAP, mitogen activated protein; TNFα, tumor necrosis factor α; IL-1β, interleukin 1β; MKK3, mitogen activated protein kinase kinase-3; MKK6, mitogen activated protein kinase kinase-6; RA, rheumatoid arthritis; ERK1, mitogen activated protein kinase 1; JNK1−3, c-Jun N-terminal kinase 1−3; MK2, mitogen activated protein kinase activated protein kinase-2; COPD, chronic obstructive pulmonary disease; TMEDA, tetramethylethylenediamine; HBTU, 2-(1*H*-benzotriazole-1-yl)-1,1,3,3-tetramethyluronium hexafluorophosphate; S-Phos, 2-dicyclohexylphosphino-2′,6′-dimethoxybiphenyl; *m*CPBA, *m*-chloroperbenzoic acid; DIEA, Hünig's base; LDA, lithium diisopropylamide; LPS, lipopolysaccharide; THP-1, human acute monocytic leukemia cell line; SAR, structure−activity relationship; HWB, human whole blood; CHO, Chinese hamster ovary; hERG, human ether-a-go-go-related gene; HEK, human embryonic kidney; AIA, adjuvant-induced arthritis; ATF2, activating transcription factor 2; RPMI, Roswell Park Memorial Institute medium

■ REFERENCES

(1) Han, J.; Lee, J. D.; Bibbs, L.; Ulevitch, R. J. A MAP kinase targeted by endotoxin and hyperosmolarity in mammalian cells. *Science* **1994**, *265*, 808−811.

(2) Raingeaud, J.; Gupta, S.; Rogers, J. S.; Dickens, M.; Han, J.; Ulevitch, R. J.; Davis, R. J. Characterization of the structure and function of a novel MAP kinase kinase (MKK6). *J. Biol. Chem.* **1996**, *271*, 2886−2891.

(3) Raingeaud, J.; Whitmarsh, A. J.; Barrett, T.; Derijard, B.; Davis, R. J. MKK3- and MKK6-regulated gene expression is mediated by the p38 mitogen-activated protein kinase signal transduction pathway. *Mol. Cell. Biol.* **1996**, *16*, 1247.

(4) Badger, A. M.; Bradbeer, J. N.; Votta, B.; Lee, J. C.; Adams, J. L.; Griswold, D. E. Pharmacological profile of SB 203580, a selective inhibitor of cytokine suppressive binding protein/p38 kinase, in animal models of arthritis, bone resorption, endotoxin shock and immune function. *J. Pharmacol. Exp. Ther.* **1996**, *279*, 1453−1461.

(5) Feldmann, M.; Brennan, F. M.; Maini, R. N. Role of cytokines in rheumatoid arthritis. *Annu. Rev. Immunol.* **1996**, *14*, 397−440.

(6) Rutgeerts, P.; D'Haens, G.; Targan, S.; Vasiliauskas, E.; Hanauer, S. B.; Present, D. H.; Mayer, L.; van Hogezand, R. A.; Braakman, T.; DeWoody, K. L.; et al. Efficacy and safety of retreatment with anti-tumour necrosis factor antibody (Infliximab) to maintain remission in Chron's disease. *Gastroenterology* **1999**, *117*, 761−769.

(7) Foster, M. L.; Halley, F.; Souness, J. E. Potential of p38 inhibitors in the treatment of rheumatoid arthritis. *Drug News Perspect.* **2000**, *13*, 488−497.

(8) (a) Kumar, S.; Boehm, J.; Lee, J. C. p38 MAP kinases: key signaling molecules as therapeutic targets for inflammatory diseases. *Nat. Rev. Drug Discovery* **2003**, *2*, 717−726. (b) Mayer, R. J.; Callahan, J. F. p38 MAP kinase inhibitors: a future therapy for inflammatory diseases. *Drug Discovery Today: Ther. Strategies* **2006**, *3* (1), 49−54.

(9) Lee, J. C.; Laydon, J. T.; McDonnell, P. C.; Gallagher, T. F.; Kumar, S.; Green, D.; McNulty, D.; Blumenthal, M. J.; Heyes, J. R.; Landvatter, S. W.; Strickler, J. E.; McLaughlin, M. M.; Siemens, I. R.; Fisher, S. M.; Livi, G. P.; White, J. R.; Adams, J. L.; Young, P. R. A protein kinase involved in the regulation of inflammatory cytokine biosynthesis. *Nature* **1994**, *372*, 739−746.

(10) (a) Weisman, M.; Furst, D.; Schiff, M.; Kauffman, R.; Merica, E.; Martin-Munley, S. FRI0018 a double-blind, placebo controlled trial of VX-745, an oral p38 MAP kinase inhibitor, in patients with rheumatoid arthritis (RA). *Ann. Rheum. Dis.* **2002**, *61* (Suppl. 1). (b) Goldstein, D. M.; Kuglstatter, A.; Lou, Y.; Soth, M. J. *J. Med. Chem.* **2010**, *53*, 2345−2353.

(11) Ferraciola, G. F. VX-745 Vertex Pharmaceuticals. *Curr. Opin. Anti-Inflammatory Immunomodulatory. Invest. Drugs* **2000**, *2*, 74−77.

(12) Haddad, J. J. VX-745 (Vertex Pharmaceuticals). *Curr. Opin. Invest. Drugs* **2001**, *2*, 1070−1076.

(13) Cohen, S. B.; Cheng, T. T.; Chindalore, V.; Damjanov, N.; Burgos-Vargas, R.; Delora, P.; Zimany, K.; Travers, H.; Caulfield, J. P. Evaluation of the efficacy and safety of pamapimod, a p38 MAP kinase inhibitor, in a double-blind, methotrexate-controlled study of patients with active rheumatoid arthritis. *Arthritis Rheum.* **2009**, *60* (2), 335−44.

(14) For further discussion on the "flip" binding mode of unrelated series, see the following: (a) Fitzgerald, C. E.; Patel, S. B.; Becker, J. W.; Cameron, P. M.; Zaller, D.; Pikounis, V. B.; O'Keefe, S. J.; Scapin, G. *Nat. Struct. Biol.* **2003**, *10*, 764. (b) Natarajan, S. R.; Heller, S. T.; Nam, K.; Singh, S. B.; Scapin, G.; Patel, S.; Thompson, J. E.; Fitzgerald, C. E.; O'Keefe, S. *J. Bioorg. Med. Chem. Lett.* **2006**, *16* (22), 5809.

(15) Fitzgerald, C. E.; Patel, S. B.; Becker, J. W.; Cameron, P. M.; Zaller, D.; Pikounis, V. B.; O'Keefe, S. J.; Scapin, G. Structural basis for p38α MAP kinase quinazolinone and pyrido-pyrimidine inhibitor specificity. *Nat. Struct. Biol.* **2003**, *10*, 764−769.

(16) Lumeras, W.; Caturla, F.; Vidal, L.; Esteve, C.; Balagué, C.; Orellana, A.; Dominguez, M.; Roca, R.; Huerta, J. M.; Godessart, N.; Vidal, B. Design, synthesis and structure-activity relationships of aminopyridine *N*-oxides, a novel scaffold for the potent and selective inhibition of p38 mitogen activated protein kinase. *J. Med. Chem.* **2009**, *52*, 5531−5545.

(17) Hunt, J. A.; Kallashi, F.; Ruzek, R. D.; Sinclair, P. J.; Ita, I.; McCormick, S. X.; Pivnichny, J. V.; Hop, C. E. C.; Kumar, S.; m Wang, Z.; O'Keefe, S. J.; O'Neill, E. A.; Porter, G.; Thompson, J. E.; Woods, A.; Zaller, D. M.; Doherty, J. B. p38 inhibitors: piperidine- and 4-aminopiperidine-substituted naphthyridinones, quinolinones, and dihydroquinazolinones. *Bioorg. Med. Chem. Lett.* **2003**, *13*, 467−470.

(18) Bao, J.; Hunt, J. A.; Miao, S.; Rupprecht, K. M.; Stelmach, J. E.; Liu, L.; Ruzek, R. D.; Sinclair, P. J.; Pivnichny, J. V.; Hop, C. E. C. A.; Kumar, S.; Zaller, D. M.; Shoop, W. L.; O'Neill, E. A.; O'keefe, S. J.; Thompson, C. M.; Cubbon, R. M.; Wang, R.; Zhang, W. X.; Thompson, J. E.; Doherty, J. B. p38 MAP kinase inhibitors: metabolically stabilized piperidine-substituted quinolinones and naphthyridinones. *Bioorg. Med. Chem. Lett.* **2006**, *16*, 64−68.

(19) Alonso-Alija, C.; Michels, M.; Schirok, H.; Schlemmer, K.-H.; Bell, J.; Fitzgerald, M. F.; Dodd, S.; Gill, A. Monocyclic Aroylpyridinones as Antiinflammatory Agents. WO03076405, September 2003.
(20) Schirok, H.; Alonso-Alija, C.; Benet-Buchholz, J.; Göller, A. H.; Grosser, R.; Michels, M.; Paulsen, H. Efficient regioselective synthesis of 6-amino-5-benzoyl-1-substituted 2(1*H*)-pyridinones. *J. Org. Chem.* **2005**, *70*, 9463−9469.
(21) (a) Manske, R. H. *Chem. Rev.* **1942**, *30*, 113. (b) Bergstrom, F. W. *Chem. Rev.* **1944**, *35*, 77. (c) Cheng, C. C.; Yan, S. *J. Org. React.* **1982**, *28*, 37.
(22) Wang, Z.; Canagarajah, B. J.; Boehm, J. C.; Kassisa, S.; Cobb, M. H.; Young, P. R.; Abdel-Meguid, S.; Adams, J. L.; Goldsmith, E. J. Structural basis of inhibitor selectivity in MAP kinases. *Structure (London)* **1998**, *6*, 1117−1128.
(23) See Supporting Information.
(24) Crystallographic coordinates for the structure of unphosphorylated p38α complexed with **21** have been deposited at the Protein Data Bank (www.rscb.org) with accession code 3MW1.
(25) Zimmiti, C. S.; Schwartz, R.; Torcellini, C. A.; Pargellis, C. A.; Madwed, J. B.; Weldon, S. M. Suppression of p38 activity in vitro and THF alpha production in vivo with BIRB-796 BS, a novel p38 kinase inhibitor. *Arthritis Rheum.* **2001**, *44*, S114.
(26) Regan, J.; Capolino, A.; Cirillo, P. F.; Gilmore, T.; Graham, A. G.; Hickey, E.; Kroe, R. R.; Madwed, J.; Moriak, M.; Nelson, R.; Pargellis, C. A.; Swinamer, A.; Torcellini, C.; Tsang, M.; Moss, N. Structure−activity-relationships of the p38α MAP kinase inhibitor 1-(5-*tert*-butyl-2-*p*-tolyl-2*H*-pyrazol-3-yl)-3-[4-(2-morpholin-4-yl-ethoxy)napthalen-1-yl]urea (BIRB-796). *J. Med. Chem.* **2003**, *46*, 4676−4686.